Biomass Conversion and Biorefinery
https://doi.org/10.1007/s13399-023-04809-2

ORIGINAL ARTICLE

Lignocellulosic biomass: synthesis of lignophenolic thermosets with simultaneous formation of composites reinforced by sugarcane bagasse fibers

Cristina Gomes da Silva[1,2] · **Bianca Groner Queiroz**[1] · **Elisabete Frollini**[1]

Received: 19 May 2023 / Revised: 10 August 2023 / Accepted: 27 August 2023
© The Author(s), under exclusive licence to Springer-Verlag GmbH Germany, part of Springer Nature 2023

Abstract
Short sugarcane bagasse fibers, an agro-residue vastly produced worldwide, with Brazil being the leading producer, were used to reinforce brittle phenolic-type thermosets formed from resins synthesized using lignosulfonate to replace phenol. Glutaraldehyde, which has a lower vapor pressure than formaldehyde, was tested in the lignophenolic resin synthesis to improve the composite processability. Both composites, Glu-SLig (C) and For-SLig (C), formed from glutaraldehyde/sodium lignosulfonate and formaldehyde/sodium lignosulfonate resins, respectively, showed a higher impact and flexural strength than their respective non-reinforced thermosets. This may be attributed to the compatibility between the lignophenolic matrix and sugarcane bagasse fibers, indicated by their nearby free surface energy density dispersive component values. Glu-SLig(C) presented impact resistance (≅20%), flexural modulus (≅45%), and Tg values higher than For-SLig(C). Lignophenolic thermoset composites formed from a high volume of plant-based materials can be an excellent alternative to materials used in non-structural applications, such as rigid packaging and automotive interior parts.

Keywords Lignosulfonate · Sugarcane bagasse · Thermoset matrices · Composites · Glutaraldehyde · Agricultural residues/by-products

1 Introduction

Lignosulfonate results from the sulfite pulping process and presents particular properties as water-soluble from the abundance of hydrophilic groups in its macromolecules, especially sulfonic groups [1, 2]. Figure 1 illustrates sodium lignosulfonate's complex functional chemical structure (**SLig**), composed of several groups, like aromatic hydroxyl, methoxyl, and aldehyde, which confers particular properties to lignosulfonate, making it versatile for application in diversified areas: as water reducers [3, 4], dispersion agent for dyes and pesticides [5–7] and dust depressors [8]. Furthermore, in the engineering field, lignosulfonate has been investigated as functional material due to compatible groups, hydrophilic and aromatic groups, to formulate phenolic resins to apply in the structured composites and adhesives [9–15], as a poliol in the synthesis of polyurethane-type polymers [14]. It finds application in various other fields, such as animal feed, stabilizer in colloidal suspensions, chelation, complexation, soil conditioning, and flotation [16, 17]. Efforts have been made to broaden the applications of lignosulfonate, including its use as a biosurfactant to aid in the enzymatic conversion of lignocellulosic fibers into fermentable sugars. [18].

The annual worldwide production of lignosulfonates stands at approximately 1.8 million tons, and these technical lignins constitute roughly 90% of the commercial lignin market [19]. Due to their wide range of applications and tendency to increase demand, lignosulfonates have become an important component of the wood biorefinery platform. They also can play a significant role in advancing the bioeconomy in various countries.

Despite being widely available almost worldwide, its use as a reagent in advanced value-added applications still needs to be on a large scale [20].

✉ Elisabete Frollini
elisabete@iqsc.usp.br

[1] Macromolecular Materials and Lignocellulosic Fibers Group, Center for Research on Science and Technology of BioResources, São Carlos Chemistry Institute, University of São Paulo, São Carlos, São Paulo, Brazil

[2] Federal University of Amazonas - Department of Physics, Manaus, Amazonas, Brazil

Published online: 31 August 2023

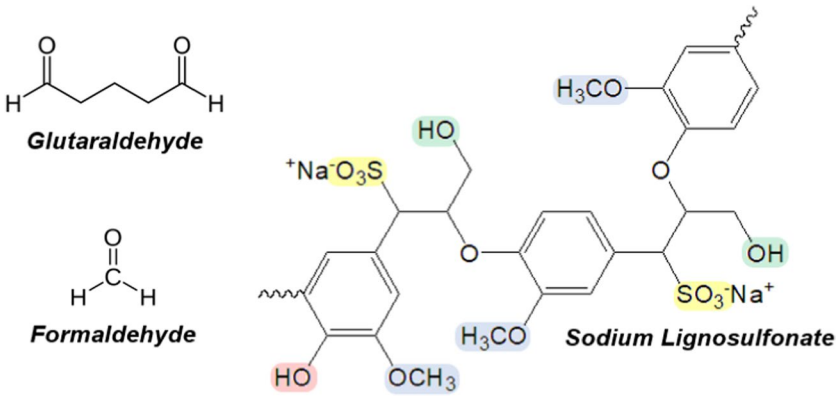

Fig. 1 Chemical structures of glutaraldehyde and formaldehyde; sodium lignosulfonate partial chemical structure

Thermosets, as the phenolic type, have been one of the most essential macromolecular materials used by industry worldwide, mainly due to their chemical and thermal properties. Biomass has the potential to replace fossil-based raw materials to meet society's growing demands for environmental sustainability [21, 22]. Chen et al. [1] reported promising results demonstrating that using SLig to prepare phenolic-type nanospheres contributed to a high-density loading of silver nanoparticles, as SLig enhanced the number of silver ions that could be adsorbed in the spheres while also preventing the aggregation of the nanoparticles.

Together with phenols, aldehydes are fundamental reagents to synthesize phenolic resins, being that formaldehyde (Fig. 1) has been used throughout the ages. Formaldehyde is in equilibrium with methylene glycol in an aqueous solution, which is its commercial form [23]. The reaction of formaldehyde with phenol forms hydroxymethyl phenols that can be later crosslinked through the formation of methylene and methyl ether bridges [24].

Glutaraldehyde (Fig. 1) has a much lower vapor pressure (16.4 mmHg at 20°C, 25% aqueous solution) than formaldehyde (33.2 mmHg at 20 °C, 37% aqueous solution) and is safer to handle. Furthermore, as a di-functional aldehyde, glutaraldehyde is an interesting candidate to substitute formaldehyde; its longer molecule can confer some flexibility to the formed networks [25].

Phenolic matrices are regularly reinforced with plant fibers, such as sisal, jute, curaua, mauve, coconut, and others [26–28]. Brazil is the leading sugarcane producer in the world. The country's raw sugar production accounts for 22% of the global output; over 750 million tons of sugarcane are produced annually [29]. This large crop leads to a relatively large amount of lignocellulosic residue in the form of sugarcane bagasse. Besides being burned to make up sugar mills' own energy needs, diverse applications have been proposed for sugarcane bagasse in the last decades, as in the production of liquid or gaseous fuels [30–32], chemicals [33–35], and materials [36, 37].

This study aimed to produce composites from a high content of renewable raw materials (Fig. 2), i.e., lignosulfonate-based phenolic matrices reinforced with sugarcane bagasse fibers (SBF) while evaluating the impact of the substitution of formaldehyde for glutaraldehyde on the properties of the thermoset matrix and the composite.

2 Materials and methods

2.1 Materials

Sugarcane bagasse fibers (SBF) were supplied by the Santa Lucia sugarcane mill (Araras, Sao Paulo, Brazil), where they were burned and ground for sugarcane processing for ethanol

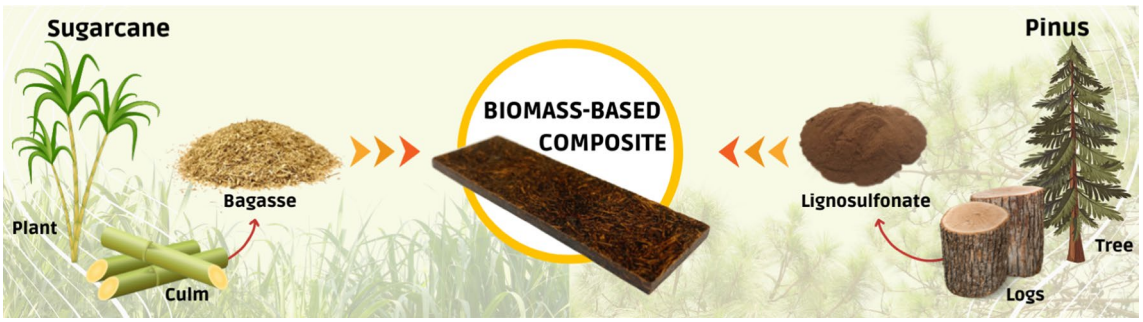

Fig. 2 Biomass-based composite: sugarcane bagasse fibers as a reinforcement of lignosulfonate-based phenolic matrix

production. First, waxes, terpenes, and fatty acids on the fiber's surface were removed by subjecting the fibers to a cyclohexane/ethanol mixture (1:1 v/v) reflux. Subsequently, the fibers were washed with distilled water and dried in an air-circulating stove at 105 °C until constant weight. The characterization of these fibers led to 56.50 ± 0.3%, 21.80 ± 0.30%, 20.90 ± 0.02% of cellulose, hemicelluloses, total Klason lignin, respectively, and 0.75 ± 0.04%, 5.50 ± 0.20%, and 47% of ashes, moisture, crystallinity, respectively, as described elsewhere [36].

The sodium lignosulfonate (**SLig**) used was a by-product obtained from the sulfite pulping processing of *Pinus taeda wood*, Vixilex SD-type (Mw approximately 6000 g mol^{-1}) composed of sulfur (5.5 wt %), magnesium (1.7 wt %), calcium (0.2 wt %), and sugars (0.9 wt %), as informed by the supplier (Borregaard Group, LignoTech (Cambará do Sul, Rio Grande do Sul, Brazil).

All other reagents, formaldehyde (Synth, 37 %), glutaraldehyde (25%, Vetec), KOH (Synth), and HCl (Synth, 37 %), were used as purchased.

2.2 Methods

2.2.1 Prepolymer synthesis

All prepolymers were synthesized by heating on a mantle using a three-necked flask coupled to a condenser with ice water circulation, a mechanical stirrer, and a thermometer, as shown in Scheme 1. The reagent proportions, Table 1, were based on a previous study [36].

Upon reaching room temperature, the solution underwent pH adjustment using concentrated HCl until pH=7. Subsequently, a rotary evaporator was utilized to remove water under reduced pressure, with a bathwater temperature of approximately 45°C.

2.2.2 Unreinforced and reinforced thermoset synthesis

Scheme 2 shows the methods for synthesizing thermosets For-SLig (T) and Glu-SLig (T), using For-SLig (P) and Glu-SLig (P), respectively, and for their corresponding SBF-reinforced composites, namely, For-SLig (C) and Glu-SLig (C), respectively. The step cycles utilized in the process were established from a previous study [36]. The length of 15 mm was used due to the typical length of sugar cane bagasse fibers produced as agricultural waste. The percentage of 30wt%, Scheme 2, was chosen based on findings from previous research [36, 37].

2.2.3 Characterizations

Prepolymers, thermosets and composites were characterized to assess their main chemical groups, thermal behavior and mechanical properties, Scheme 3. In addition, the composites' dynamic-mechanical analysis (DMA) was conducted using the TA Instruments Q800 model. The specimens, measuring 64 mm x 12 mm x 3.2 mm, were subjected to bending mode with an oscillation amplitude of 20 mm and frequency of 1 Hz. The temperature range for the analysis was from 25 °C to 200 °C, with a heating rate of 2 °C/min. Also, to visualize the morphology of fractured surfaces, scanning electron microscopy (SEM) was conducted with a Leica Model 440 (Carl Zeiss Microscopy; Jena, Germany) under the same conditions described elsewhere [37].

3 Results and discussion

3.1 FTIR

Figure 3 shows the infrared spectra of (a) sugarcane bagasse fibers (SBF) and sodium lignosulfonate (SLig);

Table 1 Proportions of the reagents in the prepolymer synthesis

Prepolymer	Aldehyde		SLig	KOH
For-SLig	Formaldehyde	1.38	1.00	0.07
Glu-SLig	Glutaraldehyde	1.00	1.00	0.07

Scheme 1 Prepolymers synthesis

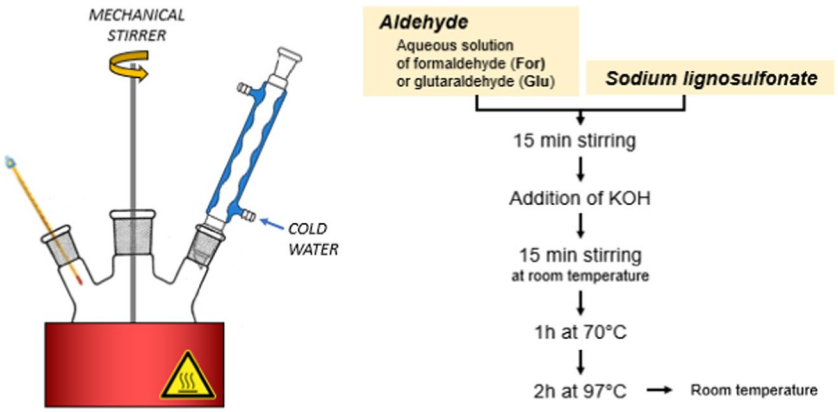

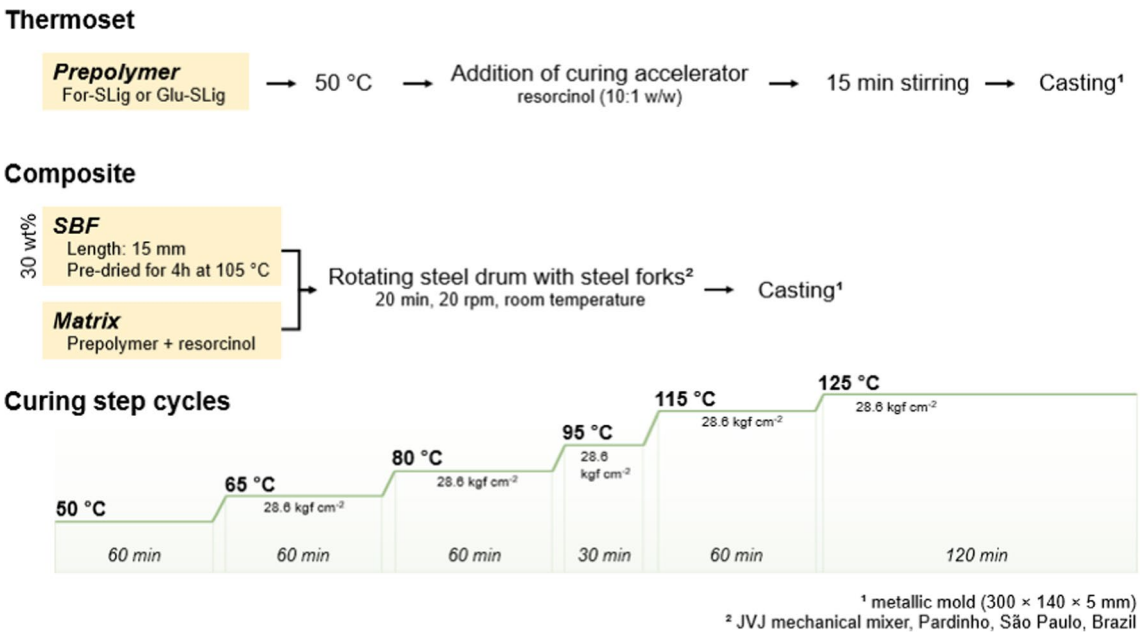

Scheme 2 Unreinforced and reinforced thermoset synthesis

Scheme 3 Characterizations of prepolymers, thermosets, and composites

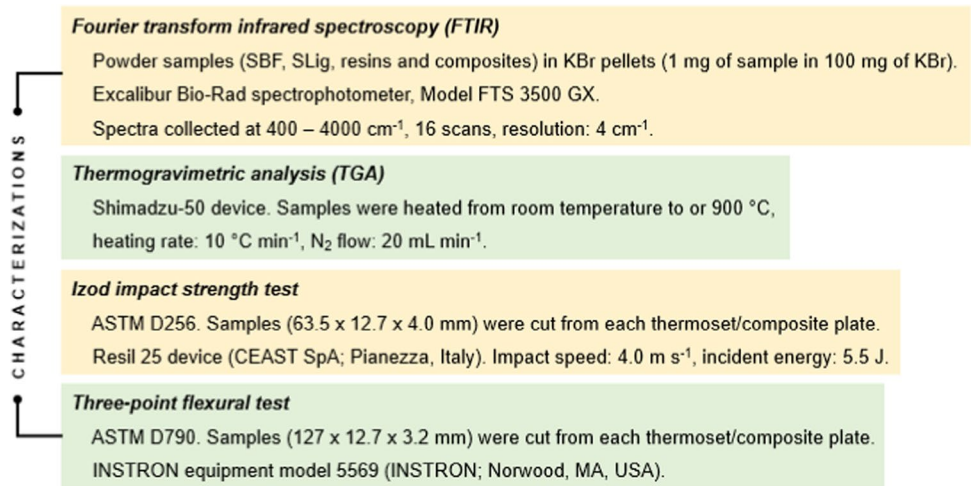

prepolymers, thermosets, and composites of (b) sodium lignosulfonate-formaldehyde (For-SLig) and (c) sodium lignosulfonate-glutaraldehyde (Glu-SLig) formulations. The large band at 3400 cm^{-1} can be attributed to the –OH group; methylene groups' C–H stretching was observed at around 2900–2980 cm^{-1}. Both bands are present in cellulose, hemicelluloses, and lignin, therefore, appeared in all spectra.

The band at 1730 cm^{-1} in the SBF spectrum (Fig. 3a) can be associated with C=O stretch in lignin and/or hemicelluloses [38]. An intense band at around 1630 cm^{-1} in the SLig spectrum (Fig. 3a) is related to C=O stretching and C=C aromatic skeleton vibrations [39], which was also present in the spectra of prepolymers, thermosets, and composites (Fig. 3b,c), where SLig replaced phenol.

The low-intensity bands at 1512 cm^{-1} and 1427-1462 cm^{-1} in the SLig spectrum (Fig. 3a) are associated with aromatic ring stretching vibrations [40]. Both bands are present in the spectra of the synthesized materials. The bands at 1250–1200 cm^{-1} were attributed to C–C, C–O, and C=O stretching [39]. The strong band around 1040 cm^{-1} can be considered a consequence of vibrations in polysaccharides: C-OH bending, C-O, and C-C stretching [41]. The band around 655 cm^{-1} is related to the vibration of sulfonate groups.

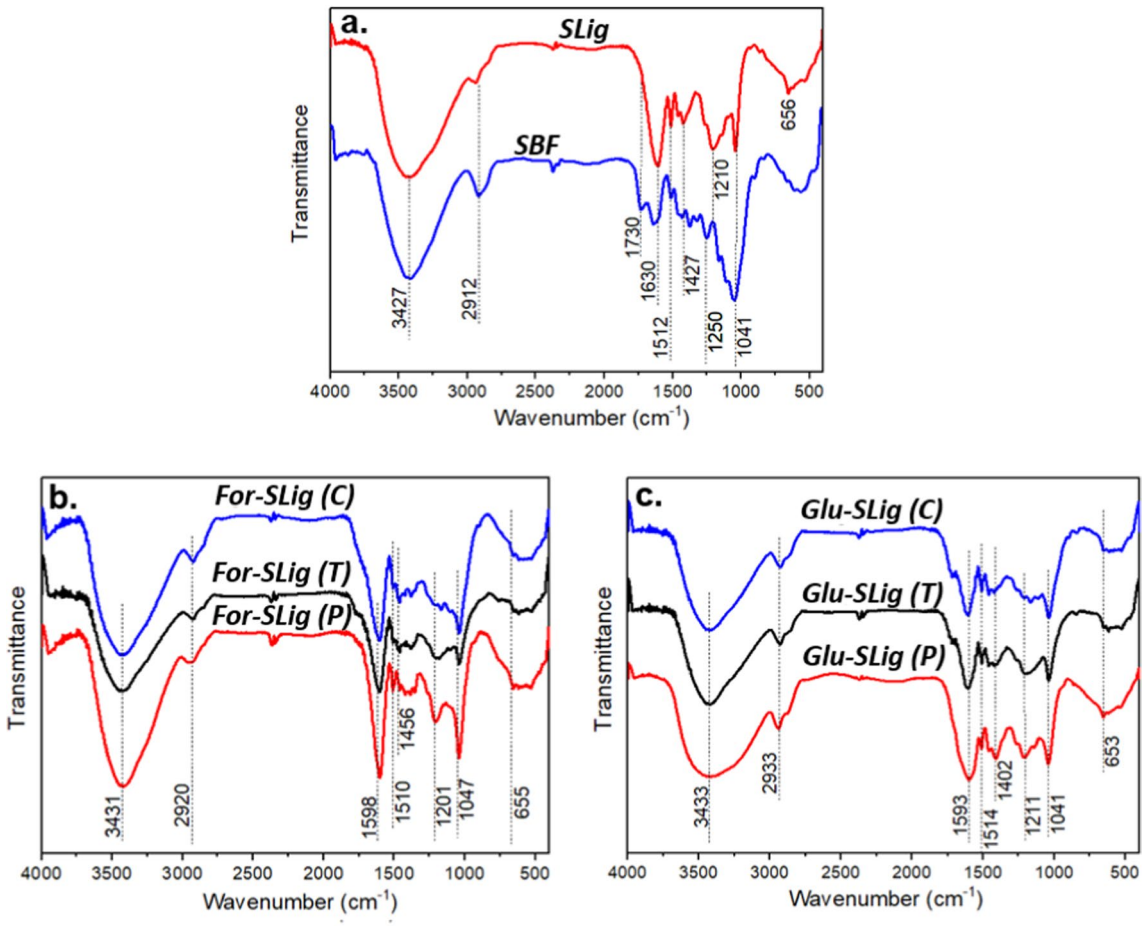

Fig. 3 FTIR spectra of **(a)** sugarcane bagasse fibers (**SBF**) and sodium lignosulfonate (**SLig**); prepolymers (**P**), thermosets (**T**), and composites (**C**) **(b)** sodium lignosulfonate-formaldehyde: **For-SLig (P), For-SLig (T), For-SLig (C),** and **(c)** sodium lignosulfonate-glutaraldehyde (**Glu-SLig**): **Glu-SLig (P), Glu-SLig (T), Glu-SLig (C)**

Figure 4 shows possible structures of the thermosets For-SLig (T) and Glu-SLig (T), which are based on the reactivity of aldehydes with phenols in an alkaline medium.

Figure 4 highlights possible bridges between the aromatic rings generated by the reaction with formaldehyde (Fig. 4a) or glutaraldehyde (Fig. 4b).

3.2 Thermal analysis

All raw materials and composites were analyzed by TGA; Fig. 5 shows the TG and DTG curves. As usually noticed for bio-based materials, there was a slight weight loss below 100 °C, corresponding to volatilization of absorbed

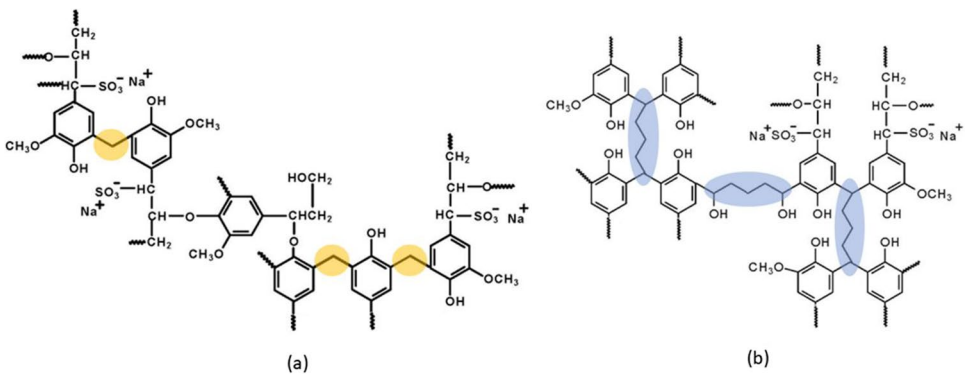

Fig. 4 Possible chemical structures of the thermosets (**a**) **For-SLig (T)** and (**b**) **Glu-SLig (T)**

or bound water [42]. Such mass loss was practically not observed for the composites For-SLig (C), Fig. 5b, and Glu-SLig (C), Fig. 5c. This suggests the surfaces of these composites are hydrophobic.

DTG curve of SLig (Fig. 5a) exhibited two intense peaks correlated to the thermal decomposition of sulfonate moieties and aromatic rings at 304 °C and 776 °C, respectively. The DTG curve of SBF (Fig. 5a) displayed a sharp peak at 364 °C and a shoulder at 331 °C, attributed to the decomposition of cellulose and hemicelluloses, respectively. SBF lignin decomposed above 530 °C.

The broad and intense peak between 120 °C and 150 °C in the DTG curves of prepolymers (Fig. 5b,c) resulted from the volatilization of the water generated as a by-product of the crosslinking reaction that occurred with the resols during scanning. However, there was no peak

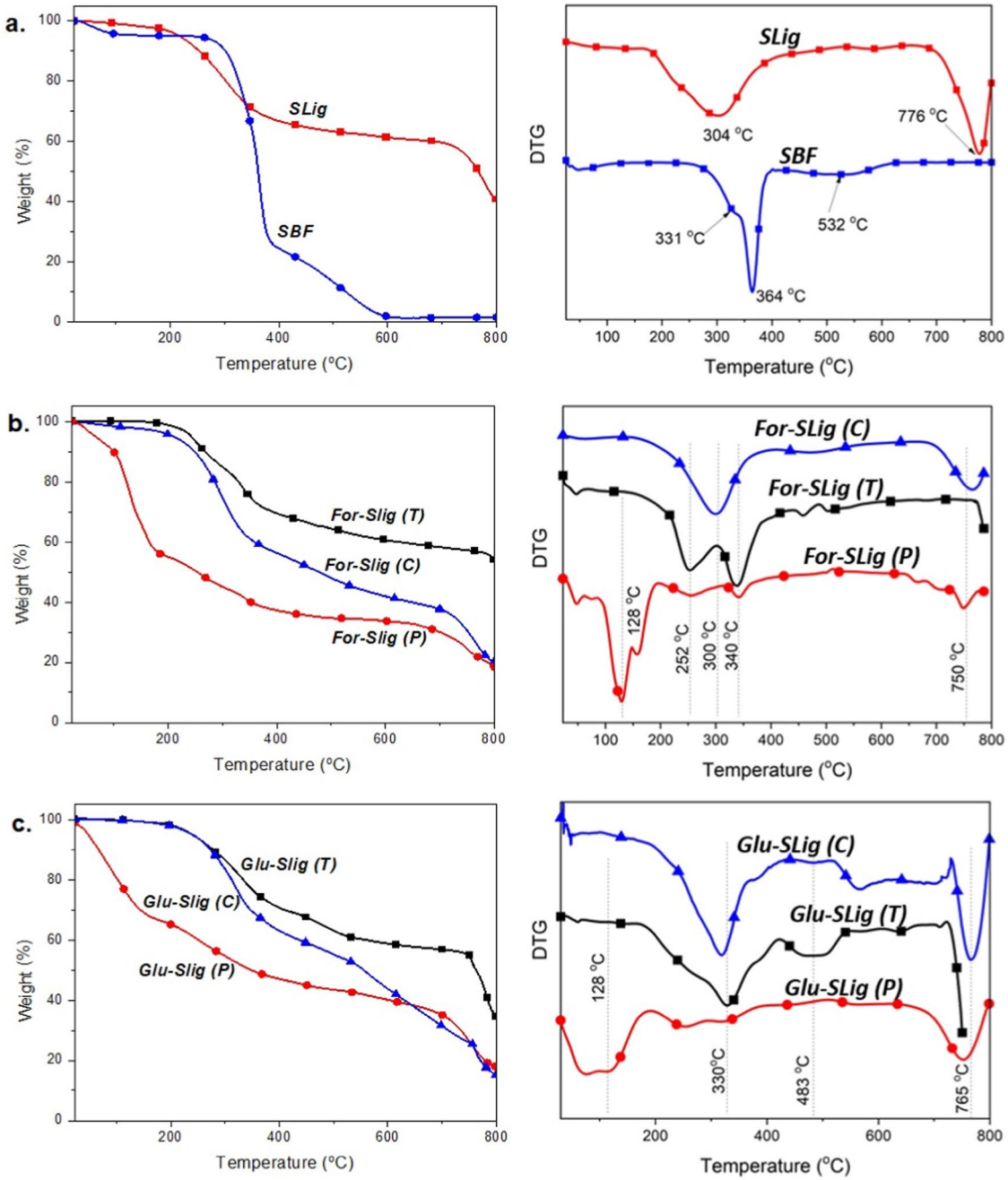

Fig. 5 TG and DTG curves of (**a**) sugarcane bagasse fibers (**SBF**) and sodium lignosulfonate (**SLig**); prepolymers (**P**), thermosets (**T**), and composites (**C**): (**b**) sodium lignosulfonate-formaldehyde: **For-SLig (P), For-SLig (T), For-SLig (C),** and (**c**) sodium lignosulfonate-glutaraldehyde (**Glu-SLig**): **Glu-SLig (P), Glu-SLig (T), Glu-SLig (C),** under N_2 atmosphere (flow 20 mL/min), and heating rate 10 °C/min)

at this temperature interval in the curves of thermosets and composites (Fig. 5b,c) because the samples were crosslinked before analyses through a gap that reached 125 °C (Scheme 2).

Between 250 °C and 350 °C, the DTG curves of the thermosets (Fig. 5b,c) shows two peaks for For-SLig (T) and a broad peak for Glu-SLig (T), which can be attributed to a residual cure step during scanning, and the consequent released and volatilization of water. This appeared as much less intense peaks in the prepolymer´s DTG curves.

Some events might be overlapped regarding the composites, such as the matrix residual cure and the thermal decomposition of the reinforcement fibers between 250 °C and 350 °C, Fig. 5. The curves for both thermosets, For-SLig (T) and Glu-SLig (T), as well as composites, For-SLig (C) and Glu-SLig (C), showed no significant differences. This means that replacing formaldehyde with glutaraldehyde did not impact the thermal stability of these materials. The peaks around 760 °C are related to the last decomposition step of the prepolymers, thermosets, and composites.

3.3 Mechanical properties

Figure 6 shows the results of the unnotched Izod impact strength for each matrix type. It should be emphasized that the thermosets proposed in this study, synthesized from lignosulfonate, formaldehyde, or glutaraldehyde, resulted in a too-fragile material, and the tests could not be performed, Fig. 6.

The phenolic-type thermosets are traditional polymeric matrices applied for a long in engineering. Its mechanical properties are usually improved by adding fibers to the matrix, and synthetic or natural fibers are commonly used to reinforce the thermoset, increasing their impact resistance [43–45], as observed for the SLig-based phenolic thermoset matrices reinforced with sugarcane bagasse fibers, Fig. 6.

The results suggested that sugarcane bagasse fibers from the Brazilian agro-industry, generated on a large scale, despite having a short length (≅1.5 mm) resulting from processing generation at the mill restraints, have potential application as reinforcement of phenolic-type composites. In addition to improving the impact strength, the bagasse residue fibers and using lignosulphonate as a reagent in the matrices synthesis resulted in composites formed from a high content of raw materials from plant sources. Besides excellent interface adhesion, the micrographs (Fig. 6 b,c) show that the matrices filled and recovered the fibers.

The substitution of formaldehyde for glutaraldehyde in the prepolymers syntheses increased the impact resistance values of the composite, reaching 82 ± 8 J m^{-1}, Fig. 6a. Fig. 6b,c shows the fractured surface of the composites. Both composites, For-SLig (C) and Glu-SLig (C) showed similar characteristics when reinforced with sugar cane bagasse: fibers broke next to the fracture plane of the matrix, the fibers were filled with resin, and few pulled-out fibers were observed.

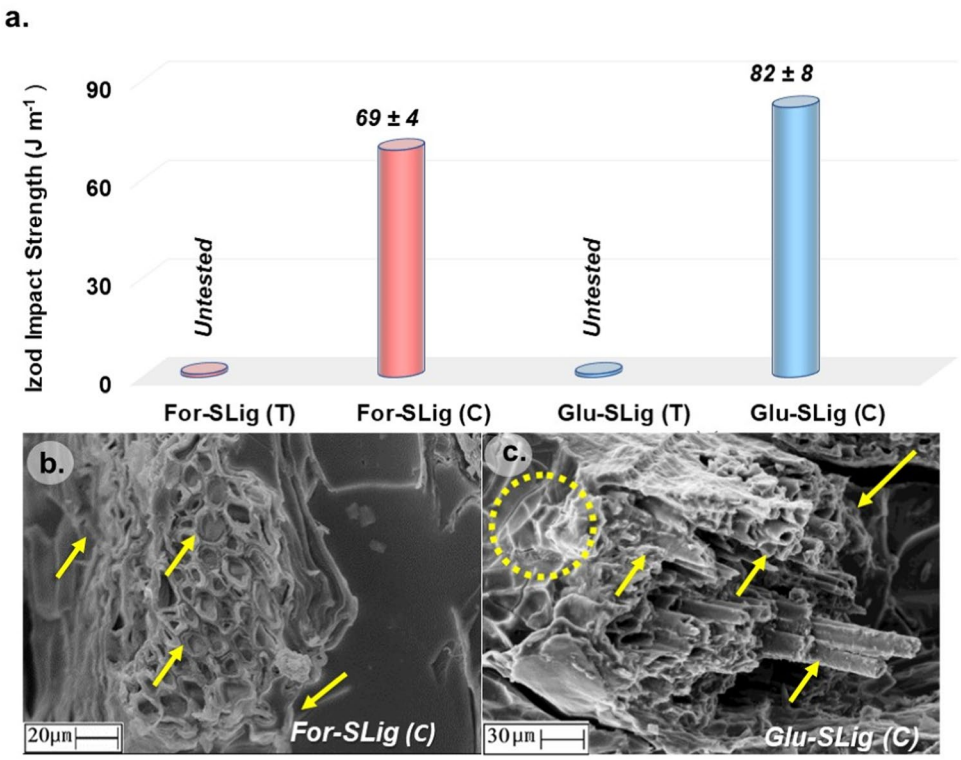

Fig. 6 (**a**) Unnotched Izod Impact test results of the lignophenolic thermosets (**T**) and composites (**C**) with sugarcane bagasse (30 wt%) as reinforcement of sodium lignosulfonate-formaldehyde (**For-SLig**) and sodium lignosulfonate-glutaraldehyde (**Glu-SLig**) matrices, (**b**) SEM micrographs of the fractured surfaces of For-Slig (**C**) and Glu-SLig (**C**)

Due to the energy transferred to the fibers from the matrices, some fibers were detached from the matrices (Glu-SLig (C), For-SLig (C), during the impact test. As shown in Fig. 4, the chemical structure of thermosets contains polar groups like hydroxyls. These same polar groups can also be found in the primary components of sugarcane bagasse fibers (lignin, cellulose, and hemicelluloses). Thus, strong hydrogen bonding interactions may occur at the fiber and matrix interface. Furthermore, the chemical structure of the matrix and lignin that make up the fibers contain non-polar domains, such as aromatic rings. These non-polar domains facilitate hydrophobic intermolecular interactions. Combined with hydrogen bonding, these interactions create good adhesion at the fiber-matrix interface.

The fibers present at the interface are hydrophilic. According to the TGA results shown in Fig. 5, the composites contain mostly hydrophobic domains on their surfaces. This helps to protect the hydrophilic fibers from absorbing water. Therefore, it can be inferred that water did not substantially impact the adhesion between the fibers and matrix [46]. Figure 6b,c illustrates the adequate interface interaction, corroborating the results of impact tests.

In Glu-SLig (C), Fig. 6c, some microcracks appeared around the fiber, which indicated that the impact load on the matrix was transferred to the fiber during the test. In this way, the energy involved in the process was distributed through the crack and absorbed by the fiber. The fiber's energy absorption partially disrupts the interactions at the fiber-matrix interface, thus causing its detachment. This mechanism is commonly related to thermoset composites due to the matrix properties [47].

The sugarcane bagasse used in the present study was produced through a process in which it is burned, as reported in 2.1. In a previous study, unburned sugarcane bagasse from mechanized harvesting and a phenolic matrix (instead of lignophenolic, as in the present study) were used. The mechanization/unburn technique enabled the incorporation of fibers of varying lengths (1/3/5 cm, 30 wt%). The impact resistance of phenolic composites reinforced with 1 cm and 3 cm fibers was around 50 J/m. Meanwhile, the composite reinforced with 3 cm fibers had an impact resistance of about 40 J/m [37]. The decrease in impact strength observed while using 5cm fibers can be attributed to the possibility of fiber bending during processing due to their length, which may negatively affect the influence of fiber length on the impact property. When comparing the best impact strength result of these phenolic composites (50 J/m, fibers measuring 1 cm and 3 cm) to the results of the present study for For-SLig (C) and GLu-SLig (C), Fig. 6, it was found that the impact strength of these lignophenolic composites were 38% and 65% higher, respectively. Based on the findings, it was observed that adding burnt fibers that are 1.5 cm in length improved the strength of lignophenolic matrices.

The composites were also tested for flexural properties, as shown in Fig. 7. The composite flexural strength of For-SLig and Glu-SLig (C) are similar; however, a noticeable increase in the flexural modulus occurred when formaldehyde was replaced by glutaraldehyde, which agrees with the higher impact strength (Fig. 6).

In previous studies on SLig phenolic thermosets [36, 48], the dispersive component of the free surface energy (which can be considered as an indication of the density of surfaces´ non-polar domains) of For-SLig thermoset, Glu-SLig thermoset, and sugarcane bagasse fibers were evaluated using inverse gas chromatography, which led to 31 mJ m^{-2}, 42 mJ m^{-2} and 45 mJ m^{-2}, respectively. It is possible to associate the better performance of Glu-SLig (C), compared to For-SLig (C), with better compatibility between the nonpolar domains of fibers and matrix, which were very close in value. Therefore, it stands out that interface plays a significant role when designing composites, and replacing formaldehyde with glutaraldehyde is beneficial when using reinforcements presenting surfaces with a higher density of nonpolar sites.

The DMA curves for the For-SLig (C) and Glu-SLig (C) composites are presented in Fig. 8. It is worth noting that the thermosets were not included in this evaluation process due to their fragile nature.

Composites DMA curves are related to matrix properties, which are impacted by the presence of fibers [46, 49]. In the present study, the matrices differ by the chemical structure of

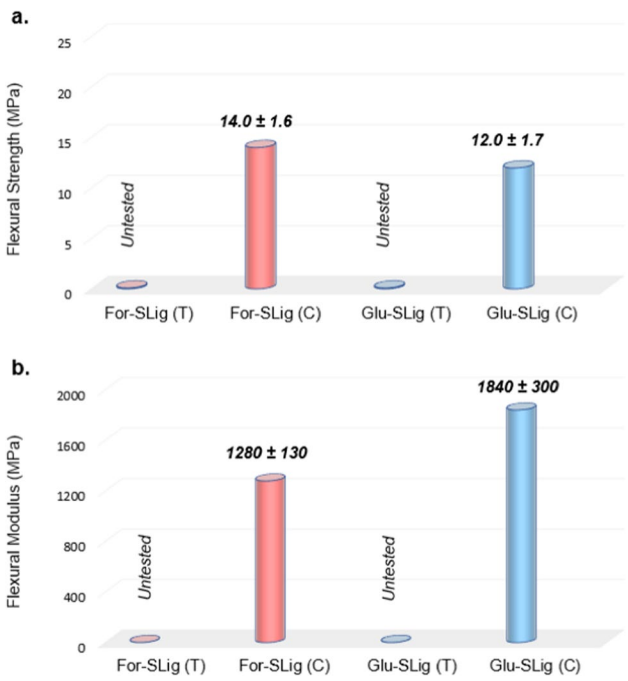

Fig. 7 (**a**) Flexural strength; (**b**) flexural modulus of lignophenolic thermosets (**T**) and composites (**C**) based on sodium lignosulfonate-formaldehyde (**For-SLig**) and sodium lignosulfonate-glutaraldehyde (**Glu-SLig**) matrices reinforced with sugarcane bagasse (30 wt%)

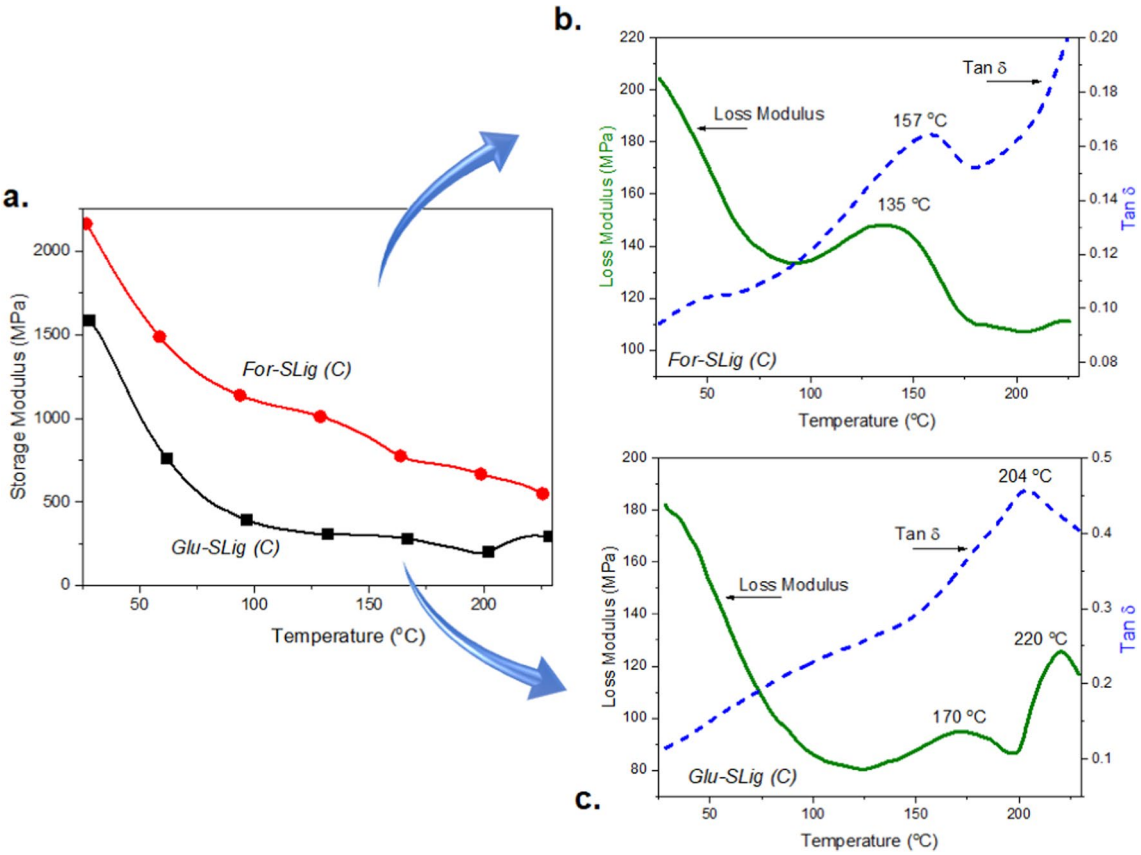

Fig. 8 (**a**) Storage modulus of the composites based on sodium lignosulfonate-formaldehyde, **For-SLig (C)**, and sodium lignosulfonate-glutaraldehyde, **Glu-SLig (C)** matrices reinforced with sugarcane bagasse (30 wt%); (**b**) and (**c**) Loss modulus and Tan δ curves of **For-SLig** and **Glu-SLig**, respectively

the bridges between the aromatic rings, Fig. 4, and both have the same reinforcement. It is worth noting that the matrices are thermosets, which are crosslinked macromolecules. As a result, the changes in the storage modulus, loss modulus, and Tan δ curves are related to the movements of uncrosslinked short segments.

Throughout the temperature range examined in Fig. 8, the storage modulus of Glu-SLig (C) is slightly lower than that of For-SLig (C). This difference may be explained, at least in part, by the fact that the bridges between the aromatic rings of Glu-SLig (C) offer less resistance to movement (a consequence of the rotation of single bonds) when compared to the methylene bridges of For-SLig (C), Fig. 4.

The peaks in the loss modulus curves, Fig. 8b,c, can be related to the glass transition, Tg, associated with the movement of many uncrosslinked segments. The Glu-SLig (C) exhibits a higher peak temperature, 170°C, than For-SLig (C), which peaks at 135°C. This can be attributed to the stronger intermolecular interaction between Glu-SLig and lignocellulosic fibers of sugarcane bagasse, as already mentioned. The restricted movement of segments in the layers closest to the fibers raises the peak temperature. Figures 8c and b highlight that the Tan δ peak temperature of Glu-SLig (C) is 204°C, which is also higher than that of For-SLig (C) at 157°C. The second peak observed in the loss modulus Glu-SLig (C) curve at 220°C could be attributed to a crosslinking during scanning. Nonetheless, it is important to highlight that this temperature is proximate to the onset of the material's thermal decomposition, evident from its TG curve (Fig. 3c).

4 Conclusions

Reinforcing the lignosulfonate-based thermosets, synthesized from glutaraldehyde or formaldehyde, with sugarcane bagasse fibers increased the flexural and impact resistance compared to unreinforced thermosets. The composite formed from the prepolymer synthesized using glutaraldehyde showed ≅20% increase in impact resistance and ≅45% increase in flexural modulus compared to the formed using formaldehyde.

The results indicated that the interactions on fiber/matrix at the interface and a consequent good adhesion between

them might arise not only using fiber modification, as primarily reported in the literature but can also be done by adjusting the matrix formulation.

A phenolic-type prepolymer was synthesized from a phenolic reagent derived from lignocellulosic biomass and an aldehyde with lower vapor pressure than formaldehyde, lignosulfonate, and glutaraldehyde, respectively. The prepolymer, previously mixed with sugarcane bagasse fibers, was used in the crosslinking reaction that led to the phenolic-type thermoset reinforced by such fibers. This process took place using molding under temperature and pressure. As a result, renewable raw materials available in various regions of the world generated composites through an uncomplicated process, facilitating the scaling up of such materials and promoting the circular bioeconomy.

Assessing the mechanical properties of composites is critical for identifying their potential applications. Based on the impact and flexural strength test results, the material can be considered suitable for use in applications involving moderate loads. In this scenario, given the excellent thermal stability at high temperatures, strong adhesion at the fiber-matrix interface, and high Tg values exhibited by the composites, they have the potential for use as internal panels in the automotive and aircraft industries, as well as in the furniture, civil construction, and rigid packaging sectors.

Authors' contributions Cristina Gomes da Silva: Conceptualization, Methodology, Formal analysis, Investigation, Data Curation, Writing - Original Draft, Writing - Review & Editing, Visualization

Bianca Groner Queiroz: Data Curation, Writing - Original Draft, Writing - Review & Editing, Visualization

Elisabete Frollini: Conceptualization, Methodology, Formal analysis, Investigation, Resources, Writing - Original Draft, Writing - Review & Editing, Visualization, Project administration, Funding acquisition

Funding CNPq (National Counsel of Technological and Scientific Development, Brazil): research productivity fellowship to E.F. (Process 309692/2017-2) and financial support (Process n° 403494/2021-4)

Data availability The manuscript provided the data set generated during the reported study.

Declarations

Ethical approval Not applicable.

Competing interests The authors declare that they have no conflict of interest.

References

1. Chen S, Wang G, Pang T, Sui W, Chen Z, Si C (2021) Green assembly of high-density and small-sized silver nanoparticles on lignosulfonate-phenolic resin spheres: Focusing on multifunction of lignosulfonate. Int J Biol Macromol 166:893–901. https://doi.org/10.1016/j.ijbiomac.2020.10.246
2. Yamini G, Shakeri A, Zohuriaan-Mehr MJ, Kabiri K (2018) Cyclocarbonated lignosulfonate as a bio-resourced reactive reinforcing agent for epoxy biocomposite: From natural waste to value-added bio-additive. J CO2 Util 24:50–58. https://doi.org/10.1016/j.jcou.2017.12.007
3. de Matos PR, Sakata RD, Foiato M, Repette WL, Gleize PJP (2021) Workability maintenance of water-reducing admixtures in high-performance pastes produced with different types of Portland cement. Rev Mater 26. https://doi.org/10.1590/s1517-707620210001.1225
4. Ouyang X, Qiu X, Chen P (2006) Physicochemical characterization of calcium lignosulfonate—A potentially useful water reducer. Colloids Surfaces A Physicochem Eng Asp 282–283:489–497. https://doi.org/10.1016/J.COLSURFA.2005.12.020
5. Qin Y, Yang D, Qiu X (2015) Hydroxypropyl Sulfonated Lignin as Dye Dispersant: Effect of Average Molecular Weight. ACS Sustain Chem Eng 3:3239–3244. https://doi.org/10.1021/acssuschemeng.5b00821
6. Yu L, Yu J, Mo W, Qin Y, Yang D, Qiu X (2016) Etherification to improve the performance of lignosulfonate as dye dispersant. RSC Adv 6:70863–70869. https://doi.org/10.1039/c6ra12173j
7. Peng R, Pang Y, Qiu X, Qian Y, Zhou M (2020) Synthesis of anti-photolysis lignin-based dispersant and its application in pesticide suspension concentrate. RSC Adv 10:13830–13837. https://doi.org/10.1039/c9ra10626j
8. Liu Y, Nie W, Mu Y, Zhang H, Wang H, Jin H, Liu Z (2018) A synthesis and performance evaluation of a highly efficient ecological dust depressor based on the sodium lignosulfonate-acrylic acid graft copolymer. RSC Adv 8:11498–11508. https://doi.org/10.1039/c7ra12556a
9. Antov P, Savov V, Mantanis GI, Neykov N (2021) Medium-density fibreboards bonded with phenol-formaldehyde resin and calcium lignosulfonate as an eco-friendly additive, Wood. Mater Sci Eng 16:42–48. https://doi.org/10.1080/17480272.2020.1751279
10. de Oliveira F, Gonçalves LP, Belgacem MN, Frollini E (2020) Polyurethanes from plant- and fossil-sourced polyols: Properties of neat polymers and their sisal composites. Ind Crop Prod 155:112821. https://doi.org/10.1016/J.INDCROP.2020.112821
11. Ghorbani M, Konnerth J, van Herwijnen HWG, Zinovyev G, Budjav E, Requejo Silva A, Liebner F (2018) Commercial lignosulfonates from different sulfite processes as partial phenol replacement in PF resole resins. J Appl Polym Sci 135:1–11. https://doi.org/10.1002/app.45893
12. Hu L, Zhou Y, Zhang M, Liu R (2012) Characterization and properties of a lignosulfonate-based phenolic foam. BioResources. 7:554–564. https://doi.org/10.15376/biores.7.1.554-564
13. Megiatto JD, Cerrutti BM, Frollini E (2016) Sodium lignosulfonate as a renewable stabilizing agent for aqueous alumina suspensions. Int J Biol Macromol 82:927–932. https://doi.org/10.1016/J.IJBIOMAC.2015.11.004
14. de Oliveira F, Ramires EC, Frollini E, Belgacem MN (2015) Lignopolyurethanic materials based on oxypropylated sodium lignosulfonate and castor oil blends. Ind Crop Prod 72:77–86. https://doi.org/10.1016/J.INDCROP.2015.01.023
15. de Oliveira F, da Silva CG, Ramos LA, Frollini E (2017) Phenolic and lignosulfonate-based matrices reinforced with untreated and lignosulfonate-treated sisal fibers. Ind Crop Prod 96:30–41. https://doi.org/10.1016/J.INDCROP.2016.11.027
16. Ruwoldt J (2020) A Critical Review of the Physicochemical Properties of Lignosulfonates: Chemical Structure and Behavior in Aqueous Solution, at Surfaces and Interfaces. Surfaces 2020(3):622–648. https://doi.org/10.3390/surfaces3040042

17. Aro T, Fatehi P (2017) Production and Application of Lignosulfonates and Sulfonated Lignin. ChemSusChem 10:1861–1877. https://doi.org/10.1002/cssc.201700082
18. Kaschuk JJ, Ferracini TV, Nitschke M, Frollini E (2023) Lignosulfonate as biosurfactant for the enzymatic conversion of sisal lignocellulosic fiber into fermentable sugars. Biomass Conv Bioref. https://doi.org/10.1007/s13399-023-04318-2
19. Gonçalves S, Ferra J, Paiva N, Martins J, Carvalho LH, Magalhães FD (2021) Lignosulphonates as an Alternative to Non-Renewable Binders in Wood-Based Materials. Polymers (Basel) 30:4196. https://doi.org/10.3390/polym13234196
20. Ganewatta MS, Lokupitiya HN, Tang C (2019) Lignin biopolymers in the age of controlled polymerization. Polymers (Basel) 11. https://doi.org/10.3390/polym11071176
21. Gallo JMR, Trapp MA (2017) The chemical conversion of biomass-derived saccharides: An overview. J Braz Chem Soc 28:1586–1607. https://doi.org/10.21577/0103-5053.20170009
22. Serrano-Ruiz JC (2020) Biomass: A Renewable Source of Fuels, Chemicals and Carbon Materials. Molecules 25:5217. https://doi.org/10.3390/molecules25215217
23. Ohra-Aho T, Rohrbach L, Winkelman JGM, Heeres HJ, Mikkelson A, Oasmaa A, Van De Beld B, Leijenhorst EJ, Heeres H (2021) Evaluation of Analysis Methods for Formaldehyde, Acetaldehyde, and Furfural from Fast Pyrolysis Bio-oil. Energy Fuel 35:18583–18591. https://doi.org/10.1021/acs.energyfuels.1c02208
24. Sarika PR, Nancarrow P, Khansaheb A, Ibrahim T (2020) Bio-Based Alternatives to Phenol and Formaldehyde for the Production of Resins. Polym 12:1–24
25. B.W. Darvell, More Chemistry, Mater. Sci. Dent (2018) 771–789. https://doi.org/10.1016/B978-0-08-101035-8.50030-4.
26. Lee CH, Khalina A, Lee SH (2021) Importance of interfacial adhesion condition on characterization of plant-fiber-reinforced polymer composites: A review. Polymers (Basel) 13:1–22. https://doi.org/10.3390/polym13030438
27. Pereira PHF, De Freitas Rosa M, Cioffi MOH, De Carvalho Benini KCC, Milanese AC, Voorwald HJC, Mulinari DR (2015) Vegetal fibers in polymeric composites: A review. Polimeros 25:9–22. https://doi.org/10.1590/0104-1428.1722
28. Rojo E, Alonso MV, Oliet M, Del Saz-Orozco B, Rodriguez F (2015) Effect of fiber loading on the properties of treated cellulose fiber-reinforced phenolic composites. Compos Part B Eng 68:185–192. https://doi.org/10.1016/J.COMPOSITESB.2014.08.047
29. FAO (2021) World Food and Agriculture – Statistical Yearbook 2021. https://doi.org/10.4060/cb4477en
30. Khodafarin R, Tavasoli A, Rashidi A (2020) Single-step conversion of sugarcane bagasse to biofuel over Mo-supported graphene oxide nanocatalyst. Biomass Convers Biorefinery:20–23. https://doi.org/10.1007/s13399-020-01037-w
31. Awais M, Li W, Munir A, Omar MM, Ajmal M (2021) Experimental investigation of downdraft biomass gasifier fed by sugarcane bagasse and coconut shells. Biomass Convers Biorefinery 11:429–444. https://doi.org/10.1007/s13399-020-00690-5
32. da Silva DDV, Machado E, Danelussi O, dos Santos MG, da Silva SS, Dussán KJ (2022) Repeated-batch fermentation of sugarcane bagasse hemicellulosic hydrolysate to ethanol using two xylose-fermenting yeasts. Biomass Convers Biorefinery. https://doi.org/10.1007/s13399-021-02199-x
33. Huong LM, Trung TQ, Tuan TT, Viet NQ, Dat NM, Nghiem DG, Thinh DB, Tinh NT, Oanh DTY, Phuong NT, Nam HM, Phong MT, Hieu NH (2022) Surface functionalization of graphene oxide by sulfonation method to catalyze the synthesis of furfural from sugarcane bagasse. Biomass Convers Biorefinery. https://doi.org/10.1007/s13399-021-02272-5
34. de Souza Queiroz S, Jofre FM, dos Santos HA, Hernández-Pérez AF, Felipe MDGDA (2021) Xylitol and ethanol co-production from sugarcane bagasse and straw hemicellulosic hydrolysate supplemented with molasses, Biomass Convers. Biorefinery. https://doi.org/10.1007/s13399-021-01493-y
35. Hernández-Pérez AF, Antunes FAF, dos Santos JC, da Silva SS, Felipe MDGDA (2020) Valorization of the sugarcane bagasse and straw hemicellulosic hydrolysate through xylitol bioproduction: effect of oxygen availability and sucrose supplementation as key factors, Biomass Convers. Biorefinery. https://doi.org/10.1007/s13399-020-00993-7
36. da Silva CG, de Oliveira F, Frollini E (2019) Sugarcane Bagasse Fibers Treated and Untreated: Performance as Reinforcement in Phenolic-Type Matrices Based on Lignosulfonates. Waste and Biomass Valorization 10:3515–3524. https://doi.org/10.1007/s12649-018-0365-z
37. da Silva CG, Frollini E (2020) Unburned Sugarcane Bagasse: Biobased Phenolic Thermoset Composites as an Alternative for the Management of this Agrowaste. J Polym Environ 28:3201–3210. https://doi.org/10.1007/s10924-020-01848-y
38. Md Salim R, Asik J, Sarjadi MS (2021) Chemical functional groups of extractives, cellulose and lignin extracted from native Leucaena leucocephala bark. Wood Sci Technol 55:295–313. https://doi.org/10.1007/s00226-020-01258-2
39. Klein SE, Rumpf J, Kusch P, Albach R, Rehahn M, Witzleben S, Schulze M (2018) Unmodified kraft lignin isolated at room temperature from aqueous solution for preparation of highly flexible transparent polyurethane coatings. RSC Adv 8:40765–40777. https://doi.org/10.1039/C8RA08579J
40. Zhou H, Yang D, Zhu JY (2016) Molecular Structure of Sodium Lignosulfonate from Different Sources and their Properties as Dispersant of TiO2 Slurry. J Dispers Sci Technol 37:296–303. https://doi.org/10.1080/01932691.2014.989572
41. Palamarchuk IA, Brovko OS, Bogolitsyn KG, Boitsova TA, Ladesov AV, Ivakhnov AD (2015) Relationship of the Structure and Ion-Exchange Properties of Polyelectrolyte Complexes Based on Biopolymers. Russ J Appl Chem 88:109–114. https://doi.org/10.1134/S1070427215010152
42. Nurazzi NM, Asyraf MRM, Rayung M, Norrrahim MNF, Shazleen SS, Rani MSA, Shafi AR, Aisyah HA, Radzi MHM, Sabaruddin FA, Ilyas RA, Zainudin ES, Abdan K (2021) Thermogravimetric analysis properties of cellulosic natural fiber polymer composites: A review on influence of chemical treatments. Polymers (Basel) 13. https://doi.org/10.3390/polym13162710
43. Caydamli Y, Heudorfer K, Take J, Podjaski F, Middendorf P, Buchmeiser MR (2021) Transparent fiber-reinforced composites based on a thermoset resin using liquid composite molding (Lcm) techniques. Materials (Basel) 14. https://doi.org/10.3390/ma14206087
44. G.S. Divya, B. Suresha, Recent Developments of Natural Fiber Reinforced Thermoset Polymer Composites and their Mechanical Properties, Indian J. Adv. Chem Sci (2016) 267–274. http://www.ijacskros.com/artcles/IJACS-2S-56.pdf.
45. Sanjay MR, Arpitha GR, Senthamaraikannan P, Kathiresan M, Saibalaji MA, Yogesha B (2019) The Hybrid Effect of Jute/Kenaf/E-Glass Woven Fabric Epoxy Composites for Medium Load Applications: Impact, Inter-Laminar Strength, and Failure Surface Characterization. J Nat Fibers 16:600–612. https://doi.org/10.1080/15440478.2018.1431828
46. Ornaghi HL, Neves RM, Monticeli FM, Thomas S (2022) Modeling of dynamic mechanical curves of kenaf/polyester composites

using surface response methodology. J Appl Polym Sci. https://doi.org/10.1002/app.52078
47. Hernandez TPA, Mills AR, Yazdani Nezhad H (2021) Shear driven deformation and damage mechanisms in High-performance carbon Fibre-reinforced thermoplastic and toughened thermoset composites subjected to high strain loading. Compos Struct 261:113289. https://doi.org/10.1016/j.compstruct.2020.113289
48. da Silva CG, Oliveira F, Ramires EC, Castellan A, Frollini E (2012) Composites from a forest biorefinery byproduct and agrofibers: Lignosulfonate-phenolic type matrices reinforced with sisal fibers. TAPPI J 11:41–49. https://doi.org/10.32964/TJ11.9.41
49. Cintil JC, Jithin J, Lovely M, Koetz J, Thomas S (2014) Nanofibril reinforced unsaturated polyester nanocomposites:Morphology, mechanical and barrier properties, viscoelastic behaviorand polymer chain confinement. Ind Crop Prod 56:246–254. https://doi.org/10.1016/j.indcrop.2014.03.005

Publisher's Note Springer Nature remains neutral with regard to jurisdictional claims in published maps and institutional affiliations.

Springer Nature or its licensor (e.g. a society or other partner) holds exclusive rights to this article under a publishing agreement with the author(s) or other rightsholder(s); author self-archiving of the accepted manuscript version of this article is solely governed by the terms of such publishing agreement and applicable law.